



Investigations of gas phase ion-molecule reactions at elevated pressures using ion mobility-mass spectrometry
by Kris E Sahlstrom

A thesis submitted in partial fulfillment of the requirements for the degree of Doctor of Philosophy in Chemistry
Montana State University
© Copyright by Kris E Sahlstrom (1997)

Abstract:

The field of gas phase ion chemistry has undergone rapid expansion during the last three decades. This has resulted in an increased need for experiments designed to elucidate the mechanisms, kinetics and thermochemistry of ion molecule reactions in the gas phase. Due to instrumental limitations, the vast majority of experimental methods operate under buffer gas pressures of less than a few Torr. Analytical methods operating at high pressures and support for theoretical models of ion-molecule reactivity are two areas that would benefit from the results from experimental methods operating under very high buffer gas pressure conditions. An Ion Mobility-Mass Spectrometer (IM-MS) has been constructed in our laboratory and has previously been applied to the study of simple substitution and clustering reactions. Modifications of the original IM-MS have increased the range of electric field strength and buffer gas pressure and have allowed the investigation of chemical systems between 300 and 1100 Torr. Rate constants for the thermal electron detachment of azulene" and for the reaction of chloride ion with methyl bromide have been measured over this pressure range. These investigations, and the reaction of chloride ion with isopropylbromide at atmospheric pressure, are the subject of this thesis work. Significant differences were observed in the behavior of these reactions when compared to results from experimental methods operating at lower buffer gas pressures. It has been determined that rate constants for the detachment of thermal electrons from azulene are inversely dependent on buffer gas pressure due to interaction of the anion with buffer gas molecules. Rate constants for the reaction of chloride ion with methylbromide were observed to increase with increased buffer gas pressure and the lifetime of the reaction intermediate was found to be in the low picosecond range. Investigations of the reaction of chloride ion with isopropylbromide revealed a change in mechanism on going from low to high buffer gas pressures. Direct bimolecular nucleophilic substitution is operative at low pressures while indirect unimolecular decomposition of the reaction intermediate was observed at high buffer gas pressures. The kinetic parameters and thermodynamic properties of this reaction at one atmosphere pressure were determined.

INVESTIGATIONS OF GAS PHASE ION-MOLECULE REACTIONS AT
ELEVATED PRESSURES USING ION MOBILITY - MASS SPECTROMETRY

by

Kris E. Sahlstrom

A thesis submitted in partial fulfillment
of the requirements for the degree

of

Doctor of Philosophy

in

Chemistry

MONTANA STATE UNIVERSITY-BOZEMAN
Bozeman, Montana

July 1997

D378
Sa 193

APPROVAL

of a thesis submitted by

Kris E. Sahlstrom

This thesis has been read by each member of the thesis committee and has been found to be satisfactory regarding content, English usage, format, citations, bibliographic style, and consistency, and is ready for submission to the College of Graduate Studies.

Eric P. Grimsrud

Eric P. Grimsrud

8/8/97
Date

Approved for the Department of Chemistry

David M. Dooley

David M. Dooley

8/11/97
Date

Approved for the College of Graduate Studies

Robert Brown

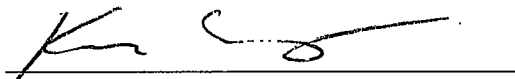
Robert Brown

8/11/97
Date

STATEMENT OF PERMISSION TO USE

In presenting this thesis in partial fulfillment of the requirements for a doctoral degree at Montana State University-Bozeman, I agree that the Library shall make it available to borrowers under rules of the Library. I further agree that copying of this thesis is allowable only for scholarly purposes, consistent with "fair use" as prescribed in the U.S. Copyright Law. Requests for extensive copying or reproduction of this thesis should be referred to University Microfilms International, 300 North Zeeb Road, Ann Arbor, Michigan 48106, to whom I have granted "the exclusive right to reproduce and distribute my dissertation in and from microform along with the non-exclusive right to reproduce and distribute my abstract in any format in whole or in part."

Signature



Date

8-11-97

ACKNOWLEDGMENT

I would like to thank the members of the research group for many hours of fruitful discussion and for their camaraderie and friendship. A particular note of appreciation goes to Dr. Berk Knighton for his invaluable technical assistance throughout this research project. The support and guidance of my research advisor, Dr. Eric Grimsrud, is gratefully acknowledged.

The successful completion of years of research, culminating in this doctoral dissertation, would not have been possible without the love and support of my family. The continued optimism and exuberance of my son, Josh, and daughter, Sabrina, provided the motivation to push ahead even in the dark nights of the Bozeman winter. I'm very thankful for the unflagging love and encouragement of my wife, Lynn, who had to contend with the sometimes onerous requirements an undertaking of this scope entailed. Finally, I'd like to thank my Mom for the spirit to pursue challenging goals in life and my Dad for the perseverance and discipline to see them through.

TABLE OF CONTENTS

	Page
INTRODUCTION.....	1
Motivations for Investigating Ion Molecule Reactions at Elevated Pressures.....	2
Experimental Support for Theoretical Models of Ion-Molecule Reactivity.....	3
Determinations of Intrinsic Chemical Behavior: Support for Models of	
Solvation.....	10
Support for Sensitive Analytical Methods.....	13
Instrumental Methods for Investigating IM Reaction in the Gas Phase.....	15
Instrumental Methods in the Low Pressure and High Pressure Range.....	17
Instrumental Methods in the Very High Pressure Range.....	20
INSTRUMENTAL DESIGN AND PRINCIPLES OF OPERATION.....	24
Instrumental Design.....	24
Ion Mobility Spectrometer.....	24
The IMS Source and Detector.....	29
The Mass Spectrometer.....	31
The Gas Handling Plant.....	32
Principles of Operation.....	33
Generation of Reagent Ions and Ionic Dynamics in the Drift Tube.....	34
Ion-Molecule Reactions in the Drift Tube.....	37
Determination of Reaction Rate Constants.....	42
Errors Analysis of Methods for Determining Rate Constants using IM-MS.....	49
THERMAL ELECTRON DETACHMENT RATE CONSTANTS FOR AZULENE ⁻ AND THE ELECTRON AFFINITY OF AZULENE AT ELEVATED PRESSURES.....	55
Experimental.....	57
Model of TED Waveforms and Waveform Analysis.....	58
Instrumental Effects on TED Waveforms.....	64
Chemical Effects on TED Waveforms.....	71
Physical and Chemical Effects of the Buffer Gas on TED Waveforms.....	74
Results and Discussion.....	78
Conclusion.....	88

TABLE OF CONTENTS - Continued

	Page
RATE CONSTANTS FOR THE GAS PHASE REACTION OF CHLORIDE ION WITH METHYLBROMIDE OVER THE PRESSURE RANGE, 300 TO 1100 TORR	89
Experimental	91
Results and Discussion	92
Conclusions	99
THE REACTION OF CHLORIDE ION WITH ISOPROPYL BROMIDE AT ATMOSPHERIC PRESSURE	100
Experimental	103
Results and Discussion	103
Reaction Modified IMS Spectra	103
Equilibrium Constants for Clustering	109
Determination of Rate Constants	119
Associated Rate Measurements at Lower Pressures	126
Enthalpy of Activation for S _N 2 Displacement within the Ion Complex	129
Conclusions	133
SUMMARY	135
LITERATURE CITED	140

LIST OF TABLES

Table	Page
1. Typical Operating Conditions Used in IM-MS	33
2. Physical Measurements, Calculated Results and Associated Uncertainties in IM-MS.....	50
3. Experimental Conditions for the Measurements of the Thermal Electron Detachment Rate Constant of Azulene ⁻	78
4. Thermal Electron Detachment Rate Constants of Azulene ⁻ Using IM-MS, PDM-ECD and PHPMS	80
5. Activation Energy and Frequency Factors for the Thermal Electron Detachment of Azulene ⁻	84
6. Thermodynamic Properties Determined by IM-MS for the Association of Chloride and Bromide Ions with Isopropyl Chloride and Isopropyl Bromide	115

LIST OF FIGURES

Figure	Page
1. Reaction coordinate diagram for a typical gas phase S_N2 nucleophilic displacement reaction. Curve A represents the energy distribution function for the reactants in thermal equilibrium with the buffer gas. Curve B represents the distribution function for entrance-channel complexes at low pressure and curve C represents the distribution function for these species at high pressure. Other major points are discussed in the text.....	4
2. Reaction coordinate diagrams for the same reaction carried out in the gas phase with an unsolvated (curve A) or monosolvated (curve B) ionic reactant, or carried out in solution (curve C).	11
3. Illustration of the various methods available for investigation of gas phase IM reactions. Limiting operating conditions of temperature and pressure are indicated.....	16
4. Diagram of the IM-MS apparatus: (A) pressure transducer, (B) needle valve, (C) rotameter, (D) source volume, (E) septum inlet, (F) insulated box, (G) Pyrex drift tube, (H) BN grid, (I) ion source, (J) pressure release valve, (K) source and drift gas exhaust, (L) mechanical vacuum pump, (M) N_2 GHP gas supply, (N) 3 inch diffusion pump, (O) fused silica capillary, (P) 4 liter stainless steel volume, (Q) mass flow controller, (R) N_2 drift gas supply, (S) first vacuum envelope, (T) second vacuum envelope, (U) 4 inch diffusion pump, (V) electrostatic lens elements, (W) Faraday plate/MS aperture, (X) on/off valve, (Y) channeltron electron multiplier, (Z) 6 inch diffusion pump, (AA) quadrupole mass filter, (BB) universal joint, (CC) drift gas inlet, (DD) N_2 source gas supply, (EE) water cooled heat exchanger (optional).....	25
5. Expanded view of the source and detector ends of the drift tube: (A) ceramic insulators, (B) electrostatic lens elements, (C) ceramic support posts, (D) stainless steel spacer post, (E) Viton O-ring, (F) drift gas entrance port, (G) Teflon washer, (H) Pyrex glass tube, (I) screen grid, (J) macor washer, (K) Faraday plate, (L) annular drift gas deflector plate, (M) BN grid, (N) drift field ring, (O) 15 mCi ^{63}Ni foil, (P) stainless steel tube.....	26

LIST OF FIGURES - Continued

Figure	Page
6. A. Ion Mobility Spectrum (IMS) and Mass Selected Ion Mobility Spectrum (MSIMS) obtained for reaction 6 with no <i>i</i> -PrBr yet added to the drift tube. MS tuned to isotopes ³⁵ Cl ⁻ and ³⁷ Cl ⁻ in the MSIMS, showing that the Cl ⁻ peak in the IMS is composed of these isotopes. B. Total mass spectrum of the contents in the drift tube obtained under the same conditions in which the Cl ⁻ ion mobility spectrum was acquired.	38
7. Ion Mobility Spectra obtained during reaction 6. Concentrations of <i>i</i> -PrBr in the drift tube are: A = 0.00, B = 2.41, C = 4.38, D = 6.60 and E = 10.77 (x10 ¹³ molec. cm ⁻³).	40
8. A. Total mass spectrum obtained by analyzing the contents of the drift tube under the conditions in which spectrum C in Figure 7 was obtained. B. Ion mobility spectrum C from Figure 7 and associated MSIMS for the ions Cl ⁻ and Br ⁻ . It can be seen that the ion mobility waveform is composed of the Cl ⁻ and Br ⁻ ion as indicated.	41
9. A. Reaction modified ion mobility waveform with 4.38 x 10 ¹³ <i>i</i> -PrBr molec. cm ⁻³ in the drift tube. Numbered lines used for determining k ₂ are explained in the text. B. Mass selected ion mobility waveforms correlating the identity and shape of the Cl ⁻ and Br ⁻ peak areas under the waveform in A.	44
10. Plot of the pseudo-first order rate constant for reaction 6 versus concentration of <i>i</i> -PrBr in the drift tube and associated least squares line.	45
11. Reaction modified ion mobility waveforms as a function of electric field strength. Spectrum A = 160, B = 144, C = 128, D = 112 and E = 96 V cm ⁻¹	47
12. Plot of ln [(A _{Cl⁻} + A _{Br⁻})/A _{Cl⁻}] vs t _d for each of the waveforms of Figure 11 with associated least squares line. Slope is equal to k ₂ [<i>i</i> -PrBr], the pseudo-first order rate constant for reaction 6.	48
13. A series of ion mobility waveforms modeled after the first-order TED of Az ⁻ . First order decay calculated with rate constants, k _d , of 600, 75 and 3 s ⁻¹ in spectra A, B and C, respectively. Total areas under each waveform are equivalent.	59

LIST OF FIGURES - Continued

Figure	Page
14. Modeled waveforms A and C from Figure 13 illustrating the methods used to determine rate constants, k_d , for first-order processes. Waveform A and resulting kinetic analysis applied at high temperatures and waveform B at lower temperatures.....	61
15. Three ion mobility waveforms corresponding to TED of Az^- at 94, 124 and 154 °C. Pressure = 740 Torr, electric field strength = 200 V cm ⁻¹	63
16. A: IMS waveforms corresponding to TED of Az^- at 144 °C under various settings of electrometer rise time. B: ln (IMS waveform) corresponding to TED of Az^- at 165 °C, slope of these plots give first order decay of source and thermally detached electrons. Signals due to source generated and thermally detached electrons are indicated. Drift tube pressure = 640 Torr, electric field strength = 144 V cm ⁻¹	67
17. A: Plot of TED first-order rate constants as a function of applied electric field. Open squares not noise reduced, filled squares noise reduced. B: Ion mobility spectra of TED of Az^- at 158 °C. Primary Y axis noise reduced, secondary Y axis not noise reduced. Pressure = 640 Torr, electric field strength in bottom mobility spectra = 144 V cm ⁻¹	69
18. Mass Spectrum and Ion Mobility Spectrum of Az^- TED at 87 °C. Pressure = 640 Torr, electric field strength = 144 V cm ⁻¹	72
19. Mass Spectrum and Ion Mobility Spectrum with associated Mass Selected Ion Mobility Spectra of Az^- TED at 160 °C. Pressure = 640 Torr, electric field strength = 144 V cm ⁻¹	73
20. Series of IMS waveforms at 164 and 102 °C at 300, 640 and 1100 Torr drift tube pressure (N ₂). Electric field strength = 200 V cm ⁻¹ at 740 and 1100 Torr and 160 V cm ⁻¹ at 300 Torr	75
21. Ion mobility spectra of Az^- TED in CH ₄ and N ₂ buffer gases at 82 and 144 °C. All spectra obtained at 740 Torr pressure and 200 v cm ⁻¹ applied electric field.	76

LIST OF FIGURES - Continued

Figure	Page
22. A series of IMS waveforms corresponding to TED of Az^- at high (166, 148 and 122 °C) and low (82, 102 and 113 °C) temperatures used in determining the rate constants for the TED of Az^- . The areas in the low temperature waveforms due to Cl^- and impurity peaks were subtracted from the areas due to $(Az^-)_0$ and $(Az^-)_t$ in determining rate constants. The high intensity Az^- peak was truncated at equal levels to reveal low level details at 82 and 102 °C.....	79
23. Az^- thermal electron detachment rate constants as a function of temperature, pressure and experimental method. Analytical expression for PHPMS is derived from Arrhenius data and given as a solid line. Open squares are PDM-ECD, filled triangles, squares and circles are IM-MS at 1100, 740 and 300 Torr, respectively.....	81
24. Arrhenius plots of the IM-MS data taken at 740 Torr in Table 4. An explanation of the two methods of analysis is given in the text. Estimated error bars included for log plot.....	83
25. Rate constants observed for the reaction of chloride ion with methyl bromide (rectangle A) and with n-butylbromide (rectangle B) by ion mobility spectrometry at 125 °C as a function of buffer gas pressure. Measurements were made using both nitrogen (open circles) and methane (solid dots) as the buffer gas.....	93
26. Reaction-modified ion mobility spectra observed at relatively high temperature, 150 °C. The reactant ion, Cl^- , is made in the ion source by electron capture to CCl_4 . The product ion, Br^- , is produced at all points along the drift tube by the reaction of Cl^- with <i>i</i> -PrBr. The concentration of <i>i</i> -PrBr added to the drift tube is indicated (in units of 10^{13} molecules/cm ³). The electric field within the drift tube is set to 144 V cm ⁻¹ . Note that the drift times of the ions are not significantly increased by the successive addition of <i>i</i> -PrBr to the drift gas at this temperature.....	104

LIST OF FIGURES - Continued

Figure	Page
27. Reaction-modified ion mobility spectra observed at relatively low temperature, 35 °C, as a function of the <i>i</i> -PrBr concentration (in units of 10 ¹³ molecules/cm ³) added to the drift gas. The electric field is 144 V cm ⁻¹ . At this temperature, the drift times of the Cl ⁻ reactant and Br ⁻ product ions are significantly increased with increased [<i>i</i> -PrBr] due to the clustering of both halide ions with <i>i</i> -PrBr. At this temperature, additional ions are also noted at drift times of about 55 and 64 msec. These two ions are formed unintentionally in the ion source and are transported through the drift region without change. The identities of the primary ions that contribute to these IMS spectra are provided by associated mass spectrometry measurements, as shown in Figure 28.	106
28. Several single-ion mass spectra for principal ions that contribute to the total ion IMS spectrum observed for condition F in Figure 27. The ion identities indicated in this figure were confirmed by parallel measurements in which the intensity of other expected ions within the ³⁵ Cl/ ³⁷ Cl and/or ⁷⁹ Br/ ⁸¹ Br isotopic cluster groups of each ion type were measured. The origins of all ions indicated here are explained in the text.	107
29. A typical measurement for the observed drift time, <i>t</i> _{obs} , for the Cl ⁻ -containing ion packet versus the concentration of <i>i</i> -PrBr added to the drift gas at a relatively low temperature, 35 °C. The dashed line indicates the <i>t</i> _{obs} values expected if only first-order clustering with <i>K</i> _{eq,1} = 3.7 x 10 ⁵ atm ⁻¹ were important, with <i>K</i> _{eq,2} assumed to be zero. The point at which the <i>t</i> _{obs} values begin to diverge from this dashed line indicates the onset of significant second-order clustering. The solid line indicates the <i>t</i> _{obs} values expected if both first- and second-order clustering are assumed to be important, with <i>K</i> _{eq,1} = 3.7 x 10 ⁵ atm ⁻¹ and <i>K</i> _{eq,2} = 2.8 x 10 ³ atm ⁻¹ . Excellent fit to all drift time measurements is then obtained.	111
30. Changes in the drift time of the Cl ⁻ /Cl ⁻ (<i>i</i> -PrBr) ion packet as a function of <i>i</i> -PrBr concentration in the drift region, plotted in the form of Equation 40. Equilibrium constants for the association of Cl ⁻ with <i>i</i> -PrBr are determined from the intercepts and the slopes of the least-squares lines thereby formed, as explained in the text.	113

LIST OF FIGURES - Continued

Figure	Page
31. Van't Hoff plots of the equilibrium constants, $K_{eq,1}$, for the association of Cl ⁻ with <i>i</i> -PrBr over the temperature range 20 - 85 °C, and for the equilibrium constants, $K_{eq,2}$, for the second-order clustering reaction, $Cl(i\text{-PrBr}) + i\text{-PrBr} \rightarrow Cl(i\text{-PrBr})_2$, over the temperature range 20 - 36 °C as determined by reaction-modified IM-MS measurements.	114
32. Drift time measurements for Cl ⁻ -containing ions observed in reaction-modified IMS spectra under conditions of relatively high <i>i</i> -PrBr concentration at 35 °C, plotted in the form of equation 42 where $W = (K_{obs} + K_{obs}K_{eq,1}[i\text{-PrBr}] - K_0 - K_1K_{eq,1}[i\text{-PrBr}])/K_{eq,1}[i\text{-PrBr}]_2$. The slope of the straight line formed by t_{obs} measurements in excess of 80 msec provides a means of determining the equilibrium constant for second-order clustering, $K_{eq,2}$	117
33. Typical reaction-modified IMS spectra from which rate constants were determined at relatively low temperature. By this procedure, the drift times of all ions are progressively increased by decreasing the electric field of the drift tube. The reaction time is defined to be equal to the drift time of the Cl ⁻ -containing ion packet. The relative contribution of the Cl ⁻ -containing ions to the IMS reaction-modified waveform is progressively increased as the reaction time is increased. Temperature is 35 °C.	120
34. Extent of Cl ⁻ -containing reactant ion loss determined by IM-MS measurements versus reaction time for several temperatures, plotted in the form of Equation 49. The slopes of the lines thereby formed provide a phenomenological second-order rate constant, $k_2' = k_2 + k_1K_{eq,1}$, at each temperature. The concentrations of <i>i</i> -PrBr used at each temperature in order of increasing temperature are 7.3×10^{14} , 4.14×10^{14} , 5.89×10^{13} , and 2.43×10^{13} molecules cm ⁻³	123
35. Phenomenological second-order rate constants, $k_2' = k_2 + k_1K_{eq,1}$, for the reaction of chloride ion with isopropyl bromide determined here (dots) by IM-MS in atmospheric pressure nitrogen buffer gas and those reported by Caldwell <u>et al.</u> (squares) by PHPMS in 4 Torr of methane buffer gas, plotted in Arrhenius form $\log k = \log A - (E_A/2.3RT)$. The estimated uncertainty of individual k_2' measurements in both studies is about $\pm 20\%$	124

LIST OF FIGURES - Continued

Figure	Page
36. First-order rate constant, k_1 , for conversion of the thermal energy ion complex, $Cl(i-PrBr)$, to Br^- -containing products determined from the present IM-MS measurements at atmospheric pressure over the temperature range 20 - 175 °C.....	130
37. Principle energy changes along the $Cl/i-PrBr$ reaction coordinate. The first three magnitudes indicated in the figure have been determined here by IM-MS measurements of rate constants, k_1 , and equilibrium constants, K_1 . These measurements place the S_N2 transition state for this reaction at 2.4 kcal mol ⁻¹ above the energy of the reactants. The enthalpy of the final products has been calculated from known thermochemical data.	132

ABSTRACT

The field of gas phase ion chemistry has undergone rapid expansion during the last three decades. This has resulted in an increased need for experiments designed to elucidate the mechanisms, kinetics and thermochemistry of ion molecule reactions in the gas phase. Due to instrumental limitations, the vast majority of experimental methods operate under buffer gas pressures of less than a few Torr. Analytical methods operating at high pressures and support for theoretical models of ion-molecule reactivity are two areas that would benefit from the results from experimental methods operating under very high buffer gas pressure conditions. An Ion Mobility-Mass Spectrometer (IM-MS) has been constructed in our laboratory and has previously been applied to the study of simple substitution and clustering reactions. Modifications of the original IM-MS have increased the range of electric field strength and buffer gas pressure and have allowed the investigation of chemical systems between 300 and 1100 Torr. Rate constants for the thermal electron detachment of azulene⁻ and for the reaction of chloride ion with methyl bromide have been measured over this pressure range. These investigations, and the reaction of chloride ion with isopropylbromide at atmospheric pressure, are the subject of this thesis work. Significant differences were observed in the behavior of these reactions when compared to results from experimental methods operating at lower buffer gas pressures. It has been determined that rate constants for the detachment of thermal electrons from azulene⁻ are inversely dependent on buffer gas pressure due to interaction of the anion with buffer gas molecules. Rate constants for the reaction of chloride ion with methylbromide were observed to increase with increased buffer gas pressure and the lifetime of the reaction intermediate was found to be in the low picosecond range. Investigations of the reaction of chloride ion with isopropylbromide revealed a change in mechanism on going from low to high buffer gas pressures. Direct bimolecular nucleophilic substitution is operative at low pressures while indirect unimolecular decomposition of the reaction intermediate was observed at high buffer gas pressures. The kinetic parameters and thermodynamic properties of this reaction at one atmosphere pressure were determined.

INTRODUCTION

The field of Gas Phase Ion Chemistry (GPIC) has undergone a period of very rapid growth in the past three decades (1-5). This has been the result of the ongoing and increasingly swift development of the electronic and vacuum technologies required for the instrumentation used in this field. This evolution has resulted in an unprecedented increase in the number of experiments and analytical applications based on processes occurring in the gas phase. Knowledge of the chemical and physical processes occurring in these gas phase environments is often essential in these applications. Thus, theoretical and experimental investigations to determine fundamental kinetic and thermochemical parameters for processes occurring in the gas phase are vital and have attended the rapid development of GPIC.

While literally thousands of papers have been published concerning ion-molecule (IM) reactions at low (< 5 Torr) buffer gas pressures, less than 20 papers have been published in which IM reactions have been investigated by instrumental methods that use buffer gases in the very high pressure (VHP) range (6 - 20). (For convenience, buffer gas pressure ranges will be divided into the low pressure (LP) range, between 10^{-7} and 10^{-5} Torr, the high pressure (HP) range, between 0.1 and 5 Torr and the very high pressure (VHP) range, between 100 Torr and 10 atmospheres buffer gas pressure). This is not due to a lack of interest in processes occurring at higher pressures, but rather due to instrumental difficulties encountered at these pressures. This lack of knowledge concerning IM reactions at VHP is an important motivation for developing new, reliable methods for investigating IM reactions under conditions of VHP.

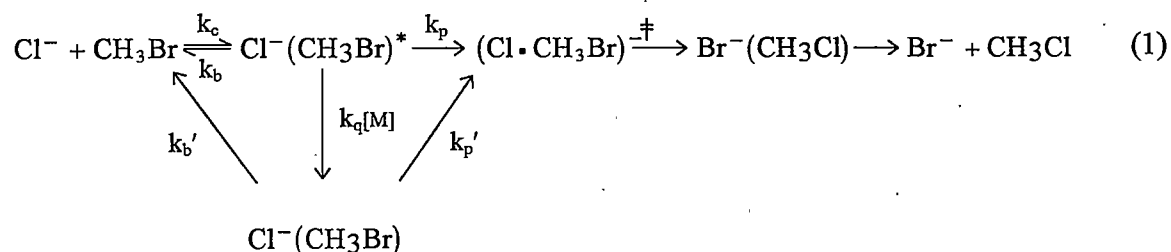
In response to this need, a new instrumental method has been developed in our laboratory which incorporates the advantages of Ion Mobility Spectrometry (IMS) and Mass Spectrometry (MS) and which shall be referred to hereafter as Ion Mobility - Mass Spectrometry (IM-MS). This instrument has previously been successfully applied to the study of simple bimolecular reactions (10) and cluster equilibria (11). Modifications to the original IM-MS have since expanded its utility to include the investigation of IM reactions over the pressure range of 300 to 1100 Torr. Rate constants for the thermal electron detachment of azulene⁻ (Az⁻) and for the reaction of chloride ion with methyl bromide (Cl⁻/CH₃Br) have both been measured over this pressure range. These investigations, and the reaction of chloride ion with isopropylbromide (Cl⁻/*i*-PrBr), are the subject of this thesis work.

Motivations for Investigating Ion Molecule Reactions at Elevated Pressures

Important motivations for the study of GPIC at VHP are the establishment of a sound experimental foundation for theories of IM reactivity at very high pressures and for models of solvation and intrinsic structure-stability and structure-reactivity relationships. Also, some of the most sensitive analytical methods used in the environmental, forensic and biological sciences rely on processes occurring in the gas phase under very high buffer gas pressures (21 - 23). Clearly, it is vital that the chemical and physical processes occurring in VHP buffer gases be understood.

Experimental Support for Theoretical Models of Ion-Molecule Reactivity

The development of instrumental methods and the expansion of computing capabilities has helped catalyze the growth of theoretical models attempting to more accurately describe IM reactivity. One of the most significant theoretical advances in GPIC and one that underlies all gas-phase nucleophilic bimolecular substitution (S_N2) reactions is the "double well" description of an IM reaction coordinate proposed by Brauman *et al.* (24) and shown in Figure 1. This reaction coordinate was invoked to explain the inefficiency of exothermic S_N2 reactions having low or negative activation energies. A typical S_N2 reaction that exhibits this behavior is the Cl^-/CH_3Br reaction system given in detail below and also shown in Figure 1.



Even though the activation barrier for this reaction is $\sim -2.0 \text{ kcal mol}^{-1}$ below the energy of the reactants, the reaction proceeds to products with only about 1% efficiency, i.e. only about 1 out of every 100 collisions results in the formation of products. The reason for this inefficiency, and the motivation for studying reactions such as these at higher buffer gas pressures, can be understood by following the progress of this reaction along the reaction coordinate in Figure 1.

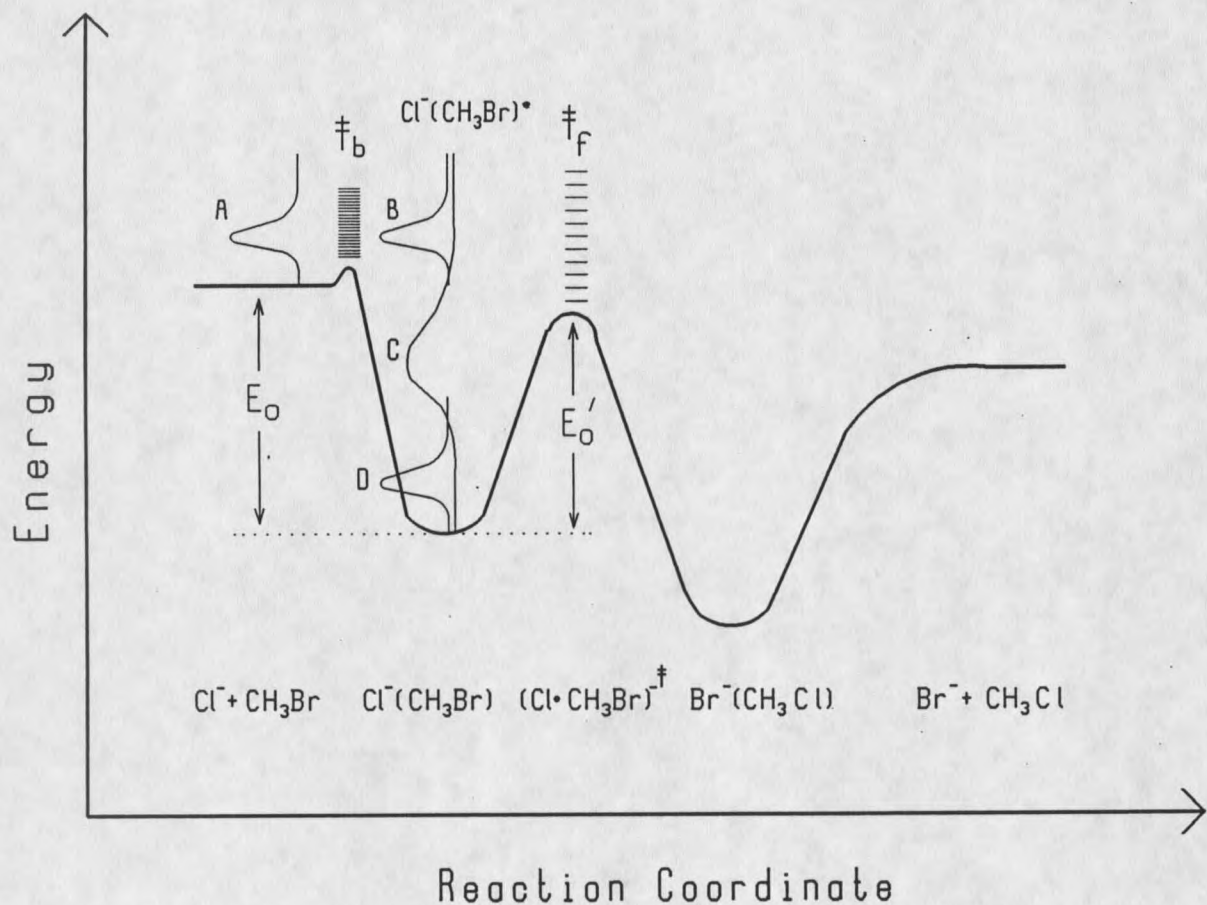


Figure 1. Reaction coordinate diagram for a typical gas phase S_N2 nucleophilic displacement reaction. Curve A represents the energy distribution function for the reactants in thermal equilibrium with the buffer gas. Curve B represents the distribution function for entrance-channel complexes at low pressure, curve C for an incompletely thermalized ensemble of complexes and curve D for the ion complexes at high pressure (completely thermalized). Other major points are discussed in the text.

The reactants, with a total energy distribution represented by curve A in Figure 1, come together with a collisional rate, k_c , described by conventional ADO theory (1), and form entrance channel ion-complexes, $\text{Cl}(\text{CH}_3\text{Br})$. This interaction involves an energy barrier due to the centrifugal forces in the $\text{Cl}(\text{CH}_3\text{Br})$ rotating ion complex, represented in Figure 1 by the first transition state, \ddagger_b . The inefficiency of the reaction is a result of competition between passage over the transition state (\ddagger_f) to products and dissociation back over the centrifugal barrier to form reactants. The observed rate constant for reaction sequence 1 depends on the magnitude of the rate constants for these two reaction pathways as shown in equation 2.

$$k_{\text{observed}} = k_c \left(\frac{k_p}{k_b + k_p} \right) \quad (2)$$

where k_p and k_b also represent k_p or k_b in reaction sequence 1. The expression in parenthesis, $k_p/(k_b + k_p)$, describes the efficiency of reaction; i.e., any reaction where k_p is large, (k_b can be ignored) is limited by the collisional rate constant, k_c . Conversely, any reaction where k_p is small is limited by the isomerization of entrance channel complexes over the transition state to form exit channel ion-complexes. The magnitude of the unimolecular rate constants in reaction sequence 1 is a function of the energy of the entrance channel ion-complexes. The ion complexes are initially formed with an excess internal energy equal to the exothermicity of the association reaction, represented by the species $\text{Cl}(\text{CH}_3\text{Br})^*$ in Figure 1 (curve B), and are said to be chemically activated. These chemically activated complexes can dissociate backwards to reactants, k_b , isomerize over the transition state to form exit channel ion-products, k_p , or

collisions with the buffer gas can remove the excess internal energy to form the ion-complex represented by the species $\text{Cl}^+(\text{CH}_3\text{Br})$. These species, referred to as thermalized ion-complexes (having thermal energy), can also form reactants or products with rates characterized by the different rate constants, k_b' and k_f' .

Whether an $\text{S}_{\text{N}}2$ reaction proceeds through chemically activated or thermal-energy ion-complexes depends on the average lifetime of the ion-complex and on the pressure of the surrounding buffer gas. If the average lifetime of the ion-complex is much shorter than the average time between collisions of buffer gas molecules (low buffer gas pressure), then the ion-complexes will retain much of their chemical activation energy, characterized by rate constants k_i . A chemical system operating under these conditions is said to be in its low pressure limit (LPL) of kinetic behavior. If the average ion-complex lifetime approaches that of the time between collisions (intermediate buffer gas pressure), then a fraction of the ion-complexes will lose their excess energy by collisions with the buffer gas molecules. The total energy distribution of the ion-complexes under these conditions might be expected to resemble curve C in Figure 1. Finally, if the average ion-complex lifetime is very long relative to the time between collisions with buffer gas molecules (very high buffer gas pressure), all of their chemical activation energy will be quenched by the buffer gas. The total energy distribution of these thermal-energy ion-complexes will then be determined by the temperature of the buffer gas, represented by the Boltzman distribution curve D in Figure 1. Under these conditions, reaction sequence 1 will proceed through the thermal-energy ion-complexes characterized by rate constants k_b' and k_p' . A reaction is said to be operating in its high pressure limit (HPL) of

kinetic behavior if the pressure of the buffer gas is high enough (or the lifetime of the ion-complex is long enough) to effectively thermalize all the ion complexes.

There are two fundamental theories for determining rate constants (k_i) for the chemically activated and thermal-energy entrance channel ion-complexes (25 - 27). The theory treating the unimolecular dissociation of the chemically activated species is referred to as RRKM (Rice, Ramsperger, Kassel and Marcus) and that for the thermal-energy species is the Transition State Theory (TST). The general expression for the unimolecular rate constant of a system in its LPL of kinetic behavior is given by equation 3

$$\text{RRKM: } k(E) = G(E - E_0) / hN(E) \quad (3)$$

where $G(E - E_0)$ is the sum of the vibrational and internal rotational quantum states for the transition state (forward or backward) in the energy range $E - E_0$ and $N(E)$ is the density of states for the entrance channel ion-complex. At a specific energy level (Figure 1), the ratio of the forward and backward rate constants is given by

$$\text{RRKM: } \frac{k_p}{k_b} = \frac{G'(E - E_0' - \Delta E_{\text{rot}})}{G(E - E_0)} \quad (4)$$

where ΔE_{rot} is a correction for the internal energy of the forward transition state to allow for conservation of angular momentum. The rate constants given here are micro-rate constants characteristic of a specific energy level; equation 4 must be integrated over an appropriate energy distribution function (i.e. ref. 25, p 240) to arrive at the overall ratio of rate constants for chemically activated reaction 1. The inefficiency of reaction 1 ($k_p/k_b < 1$) is due to the

greater number of states in the entropically favored (loose) reverse direction (dissociation) as compared to isomerization over the entropically less-favored (tight) forward transition state (Figure 1).

When an IM reaction is brought to its HPL of kinetic behavior, the unimolecular rate constant for dissociation of the ion-complex can be determined by TST, shown in Equation 5.

$$\text{TST: } k = f \frac{kT}{h} \frac{Q^\ddagger}{Q_A Q_B} e^{-E_0/RT} \quad (5)$$

Here, Q^\ddagger , Q_A , Q_B are the partition functions (electronic, vibrational, translational and rotational) of the activated complex and of reactants A and B, respectively, T is the temperature of the buffer gas and f is the transmission coefficient. The transmission coefficient is introduced to allow for the possibility of exit-channel complexes isomerizing back over the transition state and re-forming entrance channel ion-complexes. It is essentially that fraction of species crossing the transition state that go on to form products and is assumed to be unity under conditions of high buffer gas pressure (26).

While statistical methods (RRKM) of interpreting the kinetics of some reactions have been very successful (28, 29), recent theoretical and experimental evidence have indicated non-statistical (non-RRKM) behavior for some simple IM reactions. Theoretical calculations have revealed such non-statistical behavior as vibrational mode-specific rate enhancements (30 - 31), de-coupling of intra-molecular ion-complex vibrational modes (33), translational versus internal reactant energy rate differences (34) and vibrational excitation of reaction products (35).

These theoretical results have also found support in recent experiments. Graul and Bowers (36 - 37), using Mass Spectrometer based methods (~ 0.1 Torr), measured the kinetic energy distribution of the $\text{Cl}(\text{CH}_3\text{Br})^*$ ion-complex dissociation products and found vibrationally excited products. Viggiano, *et al.* (38), using a selected ion flow tube (~ 0.5 Torr), found that the rate constant for reaction sequence 1 did not depend on reactant internal energy, implying a de-coupling of the vibrational modes in the ion-complex. These theoretical and experimental results imply that statistical theories might not adequately describe some chemical systems. These uncertainties could be eliminated, and the kinetics of reaction could be reliably interpreted, if such systems could be brought to their HPL of kinetic behavior. Also, the interpretation of IM reaction kinetic data is simplified if the reaction can be brought to its HPL of kinetic behavior. In the HPL, theoretical analysis of the kinetic data requires only knowledge of the reactants and the forward, rate-determining transition state, no knowledge of entrance channel complexes or of the reverse transition state is required.

Well-established instrumental methods for investigating IM reactions, such as Ion Cyclotron Resonance and Mass Spectrometry, operate at low buffer gas pressures. Under these conditions, the ion-complexes are not expected to undergo collisions with the buffer gas and so are in their LPL of kinetic behavior. Other instrumental methods operate at high buffer gas pressures (Flowing Afterglow and Selected Ion Flow Tube) where it is difficult to predict whether or not an IM reaction is in the LPL or HPL of kinetic behavior. The IM-MS was developed in response to the need for instruments operating at very high buffer gas pressures that could force a reaction to its HPL of kinetic behavior. Also, by comparison with reaction

kinetics obtained using lower pressure methods, techniques at very high pressures could indicate whether an IM reaction was at or approaching its HPL of kinetic behavior.

Determinations of Intrinsic Chemical Behavior: Support for Models of Solvation

Theorists and physical organic chemists are interested in experimental methods that can reproduce, in the gas phase, reactions of interest in solution, so that the effects of solvation and ion-pairing on the intrinsic properties of the species involved can be determined. Two reviews of the use of GPIC as a tool for elucidating information about reactions in solution can be found written by Speranza (39) and by Bartmess (40). For this application of GPIC experiments to be valid, they must study isolated ions that have the same distribution of internal energy as in solution phase, i.e. a thermal distribution, which can be guaranteed only with complete thermalization of reacting species. While many experimental methods operating at buffer gas pressures less than about 5 Torr, such as the selected-ion flow tube (SIFT), ion cyclotron resonance (ICR) and the pulsed electron high pressure mass spectrometer (PHPMS) provide valuable information about the structure and stability of ionic intermediates, they may provide only phenomenological rate and mechanistic information rather than information characteristic of thermal (as in solution phase) species.

The effect of solvation on the reaction coordinate for a typical S_N2 reaction can be seen in the three curves in Figure 2, reproduced from Speranza (39). Curve A in Figure 2 is similar to that in Figure 1, discussed earlier, while curves B and C show the effects of increased solvation. The dramatic change in the rates of some IM reactions occurring in solution phase

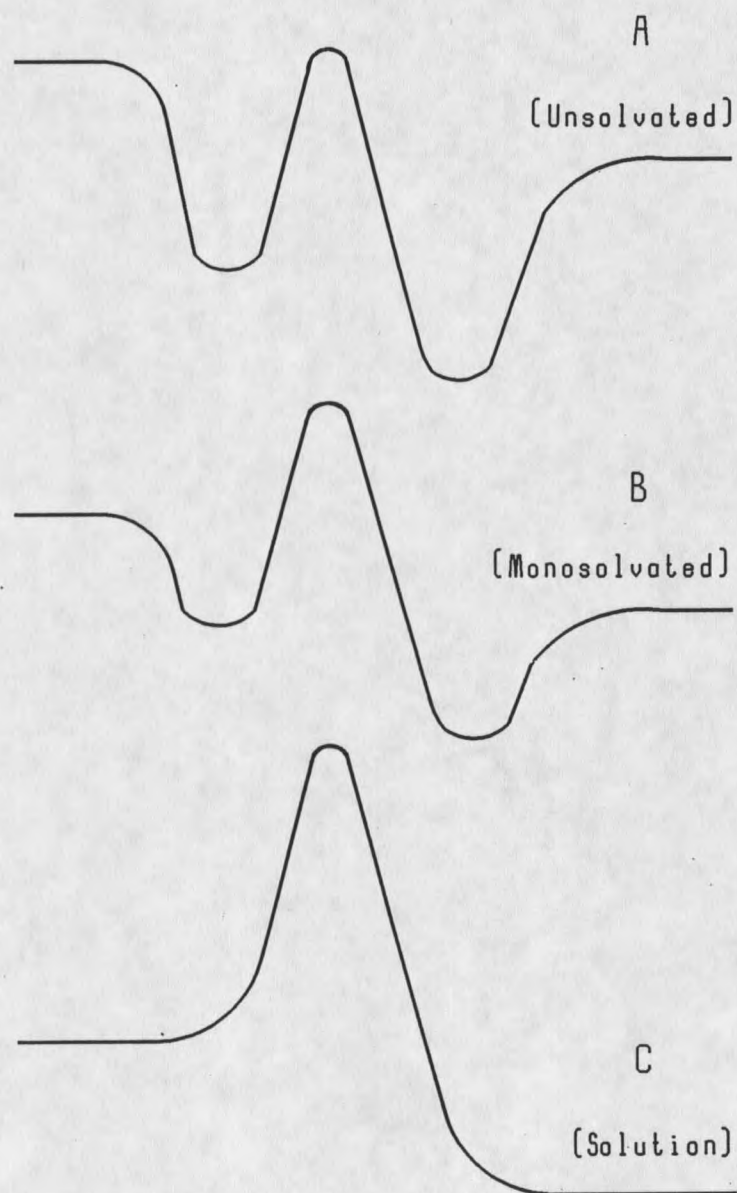


Figure 2. Reaction coordinate diagrams for the same reaction carried out in the gas phase with an unsolvated (curve A) or monosolvated (curve B) ionic reactant, or carried out in solution (curve C).

compared to the same reaction in the gas phase can be traced to the large change in the central barriers shown in Figure 2. It should be noted that large differences in reaction rates in gas phase compared to solution phase have been found only in the case of ionic (IM) reactions. For example, the rate constant for the Diels-Alder dimerization of cyclopentadiene is essentially the same in hexane or ethanol and is only three times larger than in the gas phase (41). However, it has been found that the simple S_N2 reaction, reaction 1, proceeds 15 orders of magnitude faster in the gas phase than in methanol (42).

Experiments carried out in the gas phase have also supported theories of reaction mechanisms determined from solution phase experiments. For example, it was long believed that the higher reactivity of the iodide ion relative to other halide ions in nucleophilic S_N2 reactions in solution was a consequence of the increased ability of the more polarizable iodide ion to more readily supply electron density near the substrate (24). However, studies in aprotic solvents and more recently in the gas phase have shown that the higher reactivity of the iodide ion is due to its lower degree of solvation (lower central barrier), rather than to effects caused by its higher polarizability.

The effects of solvation on the kinetics of IM reactions have been investigated by Bohme *et al.* (43) in their study of the reaction of F^- with CH_3Br and CH_3Cl and of Cl^- with CH_3Br . They found that the rate constant for the bare (unsolvated) anion (near collisional for F^- and $\approx 1\%$ collisional for Cl^-) was decreased by three orders of magnitude with the addition of just one solvent molecule to the anion and was too slow to measure with the addition of two or more solvent molecules. In aqueous solution, the rate constant for these reactions is slower by

another 15 to 16 orders of magnitude. It was also noted that the rate constant for the reaction of Cl^- with CH_3Br in the gas phase measured using their flowing afterglow apparatus (~ 5 Torr buffer gas pressure) was approximately twice the rate constant of the same reaction also measured in the gas phase, but using instead a pulsed ICR operating at much lower buffer gas pressures ($\sim 1 \times 10^{-5}$ Torr). Recent measurements by Giles and Grimsrud (10) using IM-MS (640 Torr pressure) have resulted in a rate constant for this reaction which is higher than that obtained using the flowing afterglow method. Thus, it is evident that the rate constants for IM reactions are not only different in solution and in gas phase, but are also dependent on the buffer gas pressure.

Furthering our understanding of the theory of IM reactions and providing support for models of solvation are important uses of VHP instrumental methods. Perhaps a more practical application of this technology, and an increasingly vital one, is the need to develop a better understanding of IM processes underlying some of the most sensitive analytical methods in use today.

Support for Sensitive Analytical Methods

Analytical methods operating in the VHP range can be extremely sensitive and find widespread use in the detection of trace quantities of explosives, narcotics, environmental pollutants, and for characterizing biological samples. They include Ion Mobility Spectrometry (IMS), Atmospheric Pressure Ionization Mass Spectrometry (APIMS) and Electron Capture Detection (ECD) for use with Gas Chromatography (GC). As discussed in the preceding sections, the rate constants obtained from investigations of IM reactions under low pressure

conditions are not necessarily applicable when applied to ionic reactions operating at high pressures. For example, work carried out by Knighton *et al.* (45) has shown that the APIMS spectra of C_7F_{14} were significantly altered by the addition of water or methanol at partial pressures that may also be found in the buffer gases used in the detection methods mentioned above. The APIMS spectra were altered by the formation of molecular anions clustered with the added water or methanol. It is expected that the formation of clustered species at higher pressures, particularly at low temperatures, would significantly effect the response in these detection schemes to the analyte due to the change in stability of the clustered anion. In addition, work by Mock *et al.* (46) in which the rate constant of thermal electron detachment of the azulene molecular anion, Az^- , was measured using the Photo-Detachment Modulated-ECD (PDM-ECD) at two atmospheres pressure yielded a rate constant three times lower than that measured by Kebarle *et al.* (47) using a PHPMS at 5 Torr pressure. Further measurements of the rate constants of Az^- thermal electron detachment have been carried out and reported herein using IM-MS. The results of this work revealed that the rate constants of thermal electron detachment at \sim one atmosphere pressure are higher than that reported by Mock but lower than that measured by Kebarle. This implies that increased buffer gas pressures might result in a larger equilibrium concentration of azulene adducts that are more stable than the unclustered anion. The effects and implications of azulene electron detachment using IM-MS will be discussed in more detail later.

The formation of adducts and dimers at the very high buffer gas pressures in IMS has been observed to significantly alter ion mobility spectra. Eiceman *et al.* (48) reported peak

distortion and baseline perturbations in the ion mobility spectra of butyl acetate isomers. Fragmentation of the iso-, tert- and sec- butyl acetate isomers and declustering of the n-butyl acetate isomer from the dimer to the monomer ions was observed at high (160 °C) temperatures. Preston *et al.* (49) observed the change in reduced ion mobility as a function of neutral reagent concentration in the ion mobility spectra of DPM/acetone (DPM = 3-(3-methoxypropoxy)propanol (dipropylene glycol monomethyl ether), acetone/water and pyridine/water. A decrease in the reduced mobility (longer observed drift times) as the neutral reagent (acetone or water) concentration was increased was attributed to the establishment of a clustering equilibrium in the drift tube. It was also possible to determine the thermodynamic constants for these clustering reactions by measuring the change in reduced mobility as a function of neutral reagent. Thermodynamic constants for the dimerization of pyridine were determined in this manner. Investigations of this type reveal the uncertainties inherent in the interpretations of ion mobility spectra. Clearly, these complicating effects of VHP buffer gases need to be investigated and understood.

Instrumental Methods for Investigating IM Reactions in the Gas Phase

The temperature and pressure ranges used in IM-MS and in other instrumental methods in GPIC are illustrated in Figure 3 (39). It is evident from Figure 3 that most techniques for investigating IM use low to high buffer gas pressures where chemically activated, rather than thermalized, ion-complexes are likely. A brief review of the instrumental methods illustrated in Figure 3 will reveal some of the advantages and disadvantages of methods operating under low and high buffer gas pressures.

